ACS OMEGA

http://pubs.acs.org/journal/acsodf

Article

In Vivo Antihypertensive Activity and UHPLC-Orbitrap-HRMS Profiling of *Cuphea ignea* A. DC.

Walaa M. Ismail,* Shahira M. Ezzat, Aliaa E.M.K. El-Mosallamy, Kadriya S. El Deeb, and Ahlam M. El-Fishawy

Cite This: *ACS Omega* 2022, 7, 46524−46535

Read Online

ACCESS | Metrics & More | Article Recommendations

ABSTRACT: *Cuphea ignea* A. DC. is an ornamental tropical plant belonging to the family Lythraceae. The aim of this study is to verify the *in vivo* antihypertensive potential of *C. ignea* A. DC. and to explore its metabolic profile using a UHPLC-Orbitrap-HRMS technique. The results revealed that the ethanolic extract of the leaves in two doses (250 and 500 mg/kg b.wt.) significantly normalized the elevated systolic blood pressure in N(G)-nitro-L-arginine-methyl ester-induced hypertension in rats. An angiotensin-converting enzyme (ACE) concentration was significantly decreased by the high dose extract compared to lisinopril. Nitric oxide (NO) level was significantly restored by both doses. Concerning the oxidative stress parameters, both doses displayed significant reduction in malondialdehyde (MDA) level while the high dose restored elevated glutathione level. These biochemical results were clearly supported by the histopathological examination of the isolated heart and aorta. A UHPLC-Orbitrap-HRMS study was represented by a detailed metabolic profile of leaves and flowers of *C. ignea* A. DC., where 53 compounds were identified among which flavonoids, fatty acids, and hydrolysable tannins were the major identified classes. This study established scientific evidence for the use of *C. ignea* A. DC., a member of genus *Cuphea* as a complementary treatment in the management of hypertension.

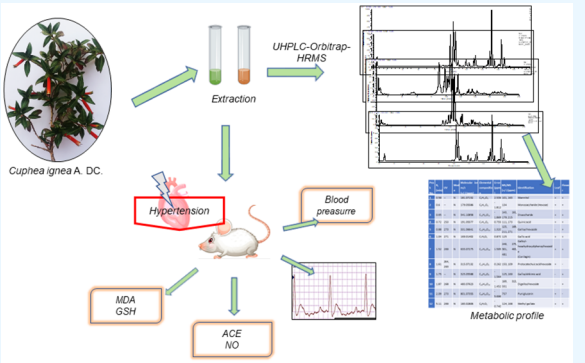

1. INTRODUCTION

Hypertension is the elevated arterial blood pressure, which can cause severe complications as heart diseases, stroke, and some kidney diseases. High blood pressure can be attributed to a number of causes, including increased activity of renin−angiotensin system (RAS), sympathetic responses, and genetic factors.[1] Several mediators contribute in controlling blood pressure besides the renin−angiotensin system (RAS), including nitric oxide levels and oxidative stress.[2] RAS is a physiological mechanism that regulates blood pressure, in which the renin enzyme converts angiotensinogen into angiotensin I.[3] An angiotensin-I-converting enzyme (ACE) manages the conversion of angiotensin I to angiotensin II and inactivates the vasodilator bradykinin. Angiotensin II exerts potent vasoconstrictor activity, while nitric oxide (NO) is a potent direct vasodilator that acts as a functional antagonist to angiotensin II action on vascular tone, and it also decreases the production of ACE. Consequently, it plays a major role in regulating blood pressure.[2]

Reactive oxygen species (ROS) also play a role in altering blood pressure due to their impact on decreasing nitric oxide (NO) bioavailability.[2] Reactive oxygen species are extensively increased in hypertensive patients as a result of activated nicotinamide adenine dinucleotide phosphate (NADPH) oxidase by angiotensin II. Consequently, ROS are accumulated and act to scavenge NO. Accordingly, it will be very effective to explore an antihypertensive drug that possesses additional antioxidant effects.[4]

Traditionally, *Cuphea* has been widely used for the treatment of cardiovascular disorders, including arterial hypertension and heart diseases.[5,6] The ethanolic extract of the aerial parts of *Cuphea carthagenensis* (Jacq.) J.F.Macbr. showed ACE inhibition and vasorelaxant activities.[7,8] These reported antihypertensive activity for a member of the genus encouraged us to explore another candidate, i.e., *Cuphea ignea* A. DC. for its possible activity in the management of hypertension.

C. ignea A. DC. is an ornamental plant distributed in the tropical zone.[9] Previously and as a preliminary essential step in

Received: August 20, 2022
Accepted: November 24, 2022
Published: December 9, 2022

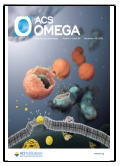

testing the plant, *in vitro* antihypertensive activities were applied and different extracts were proved to possess significant *in vitro* inhibition of ACE and renin enzymes, in addition to the strong antioxidant activities, especially the ethanolic extract of the leaves.[9] Nanoformulation of *C. ignea* A. DC. extract of the leaves effectively inhibited SARS-CoV-2 virus *in vitro* with the identification of 15 phenolic compounds using the HPLC technique.[10] Several phenolic compounds including flavonoids and phenolic acids were also reported in the plant.[10,11]

The present study aimed to investigate the *in vivo* antihypertensive effect of the ethanolic extract of *C. ignea* A. DC. leaves compared to lisinopril as a reference standard antihypertensive drug in male Sprague−Dawley rats. Induction of hypertension was carried out using nitro-L-arginine-methyl ester (L-NAME), a well-known method used for induction of hypertension by decreasing NO synthesis. In the L-NAME-induced hypertension model, oxidative stress markers are extensively increased, *e.g.*, malondiadehyde (MDA), which is an indicator for lipid peroxidation. A significant decrease in the level of natural antioxidants such as reduced glutathione (GSH) could also be observed.[2] Accordingly, in the current study, blood pressure and electrocardiography were recorded, in addition to measurements of ACE and NO levels. Oxidative stress markers, including malonaldehyde (MDA) and glutathione (GSH), were also measured. Histopathological examination of the isolated heart and aorta was undertaken.

Additionally, the metabolite profile of the leaves and flowers of the plant was explored using a UHPLC-Orbitrap-HRMS technique to provide detailed insights into the chemical constituents of the plant and to shed light on the constituents contributing to the antihypertensive activity of the *C. ignea* A. DC. leaves.

2. MATERIALS AND METHODS

2.1. Chemicals, Reagents, and Biochemical Kits. Rat angiotensin-converting enzyme (ACE) ELISA kit was purchased from Cusabio, Houston. Lisinopril was obtained from Global Napi Pharmaceuticals, Cairo, Egypt. N(γ)-nitro-L-arginine methyl ester (L-NAME), vanadium trichloride, absolute ethanol, malondialdehyde (MDA), Ellman's reagent, sodium nitrite, sulfanilamide, thiobarbituric acid, trichloroacetic acid, and *N*-(1-naphthyl)ethylenediamine dihydrochloride (NEDD) were all obtained from Sigma-Aldrich, St. Louis, Missouri. Dipotassium hydrogen phosphate and potassium dihydrogen phosphate were purchased from Sisco, India. Tween 80, umbelliferone, and LC-MS-grade analysis solvent were obtained from Sigma-Aldrich, Germany. All other chemicals used were of highest analytical grade.

2.2. Plant Material. Samples of *C. ignea* A. DC. were collected in the flowering stage in May 2015 from El Kanater El Khayreya, Egypt, and were kindly identified by Dr. Mohamed El-Gebali, a senior botanist at El-Orman Botanic Garden, Egypt. A voucher specimen (No. 4-5-2016-1) was kept in the Herbarium of Pharmacognosy department, Faculty of Pharmacy, Cairo University, Giza, Egypt.

2.3. Preparation of Extracts. *2.3.1. Ethanolic Extract of Leaves.* The air-dried powdered leaves (80 g) were extracted with 95% ethanol by cold maceration till exhaustion (6 mL × 500 mL). The ethanolic extracts were separately evaporated under reduced pressure till dryness at a temperature not exceeding 50 °C to give 9 g of dry residue of the leaves. Dilutions of the extracts were prepared in distilled water using 0.05% Tween 80 and saved for the biological study.

2.3.2. Extracts for UHPLC-Orbitrap-HRMS Analysis. The air-dried powdered leaves and flowers (120 mg each) were extracted by homogenization with 5 mL of methanol containing 10 μg/mL umbelliferone as an internal standard using sonication (20 min). The extract was vigorously vortexed and centrifuged at 10 000 rpm for 5 min and then 1 mL was filtered through a 22 μm millipore filter, followed by the injection of the filtrate in the UHPLC instrument.[12]

2.4. Animals. Forty male Sprague−Dawley rats weighing 150−170 g were brought from the animal house at the National Research Centre, Giza, Egypt, and kept for one week in the laboratory before testing under standard conditions (room temperature 24−27 °C and 60 ± 10% humidity) with alternating 12 h light and dark cycles. The diet was laboratory pellets (20% proteins, 5% fats, and 1% multivitamins) with water. All animal procedures and handling were performed according to the protocol (number MP 2550) approved on 25 November 2019 by the Research Ethical Committee of the Faculty of Pharmacy, Cairo University, Giza, Egypt.

2.5. Determination of the Safety of the Ethanolic Extract of the Leaves. The safety of the ethanolic extract of the leaves of *C. ignea* A. DC. was examined according to the OECD 425 guidelines[13] using 20 male Sprague−Dawley rats divided into four groups. The first three groups were given increased oral doses ranging from 200 to 600 mg/kg b.wt. of the ethanolic extract of *C. ignea* A. DC. The fourth group received distilled water. Animals are observed periodically during the first 24 h and daily for 14 days. Neither toxicity nor mortality was recorded in any group. Thus, the *C. ignea* A. DC. ethanolic extract of the leaves was considered safe up to 5 g/kg b.wt. It is estimated that the therapeutic doses would be 1/10 and 1/20 of the maximum soluble dose. Accordingly, doses that were used in the *in vivo* studies were 500 and 250 mg/kg b.wt. for the tested plant extract.

2.6. Experimental Design. Male Sprague−Dawley rats (150−170 g, n = 25) were distributed in random way into five groups (n = 5), and the following protocols were done over 6 weeks orally, where the first group (normal control) was given only distilled water orally for 6 weeks. The second group (hypertensive control) received L-NAME (50 mg/kg/day) in distilled water. The third (reference group) was given L-NAME (50 mg/kg/day) + lisinopril (10 mg/kg/day) in distilled water. The fourth group was given L-NAME (50 mg/kg/day) + the ethanolic extract of leaves of *C. ignea* A. DC. (250 mg/kg b.wt.) suspended in distilled water. Finally, the fifth group was given L-NAME (50 mg/kg/day) + the ethanolic extract of leaves of *C. ignea* A. DC. (500 mg/kg b.wt.) suspended in distilled water.

2.7. Blood Pressure Measurements. Systolic blood pressure (mmHg) was measured after 6 weeks for the rats by the tail-cuff technique.[14] All animals were pretrained by placing the restraining tubes in the animal cages for 20 min/day for 5 days before measurement. The tail cuff was connected to a pulse transducer that was connected to an ML 125 NIBP amplifier (ADInstruments, Australia). Systolic blood pressure was recorded, and data were analyzed using the PowerLab data acquisition system and LabChart 7.3 software (ADInstruments, Australia).

2.8. Electrocardiography (ECG) Determination. After 6 weeks of treatment, rats were anesthetized with intraperitoneal injection with thiopental (50 mg/kg) and ECG was determined.[15] The ECG signals were recorded for 1 min

https://doi.org/10.1021/acsomega.2c05356
ACS Omega 2022, 7, 46524−46535

Table 1. Effect of the Ethanolic Extract of *C. ignea* A. DC. Leaves on Systolic Blood Pressure, ACE, NO, MDA, and GSH Levels in L-NAME-Induced Hypertensive Rats[a]

group	systolic blood pressure (mmHg)	ACE (pg/mL) ± SE	NO (μmol/mL) ± SE	MDA (nmol/mL) ± SE	GSH (μmol/mL) ± SE
normal control	103.6[c] ± 5.7	251.9[c] ± 8.7	75.4[c] ± 7.2	1.5[c] ± 0.1	10.6[c] ± 0.4
hypertensive control	145.9[b] ± 7.1	288.8[b] ± 6.0	37.2[b] ± 3.4	3.2[b] ± 0.3	7.3[b] ± 0.1
lisinopril	108.6[c] ± 3.1	254.7[c] ± 5.1	65.5[c] ± 4.0	1.7[c] ± 0.2	9.5[c] ± 0.4
ethanolic extract 250 mg/kg	120.9[c] ± 4.0	270.9 ± 6.0	64.1[c] ± 7.1	2.2[c] ± 0.3	8.1[b] ± 0.1
ethanolic extract 500 mg/kg	114.6[c] ± 6.7	261.6[c] ± 2.4	67.5[c] ± 7.9	2.0[c] ± 0.2	9.2[c] ± 0.9

[a]Each value was expressed as mean ± SE, $n = 5$. [b]Significantly different from the normal group. [c]Significantly different from the hypertensive control group at $p < 0.05$.

Table 2. Effect of the Ethanolic Extract of *C. ignea* A. DC. Leaves on ECG Parameters in L-NAME-Induced Hypertensive Rats[a]

group	RR interval (s) ± SE	PR interval (s) ± SE	QRS interval (s) ± SE
normal control	0.1654[c] ± 0.0036	0.0439[c] ± 0.0013	0.0180[c] ± 0.0007
hypertensive control	0.2316[b] ± 0.0151	0.0563[b] ± 0.0017	0.0228[b] ± 0.0009
lisinopril	0.1776[c] ± 0.0046	0.0445[c] ± 0.0011	0.0185 ± 0.0005
ethanolic ext. 250 mg/kg	0.1962 ± 0.0161	0.0473[c] ± 0.0007	0.0194 ± 0.0008
ethanolic ext. 500 mg/kg	0.1783[c] ± 0.0125	0.0461[c] ± 0.0010	0.0189 ± 0.0002

[a]Each value was expressed as mean ± SE, $n = 5$. [b]Significantly different from the normal group. [c]Significantly different from the hypertensive control group at $p < 0.05$.

using ML785 PowerLab 8SP (ADInstruments, Australia) and LabChart 7.3 software (ADInstruments, Australia).

2.9. Determination of Serum Angiotensin-Converting Enzyme (ACE) Concentration. An angiotensin-converting enzyme concentration was estimated using rat angiotensin-converting enzyme (ACE) ELISA kit from Cusabio, Houston, according to the manufacturer's protocol based on the competitive inhibition enzyme immunoassay technique. A standard curve was constructed by plotting the absorbance on *y*-axis against the ACE concentration (pg/mL) on *x*-axis with concentrations ranging from 156 to 2500 pg/mL. The standard curve was used to determine the ACE concentration (pg/mL) in the samples.

2.10. Determination of Serum Nitric Oxide (NO) Concentration. Nitric oxide (NO) is a free radical that rapidly decomposes into nitrite and nitrate in biological systems. These stable breakdown products can be measured as an indication of nitric oxide levels *in vivo*.[16] The nitric oxide level in serum was determined,[17] expressed as μmol/mL and calculated using the standard calibration curve of concentrations ranging from 1.562 to 200 μmol/mL.

2.11. Determination of Malondialdehyde (MDA). Malondialdehyde (MDA) levels were determined by the method,[18] which depends on the reaction of thiobarbituric acid (TBA) with MDA at 95 °C for 45 min in acidic medium to form a thiobarbituric acid reactive product. The level of malondialdehyde in liver homogenate was calculated as nmol/mL using the standard calibration curve of serial dilutions of MDA in concentrations ranging from 0.78 to 6.26 nmol/mL.

2.12. Determination of Glutathione (GSH). GSH was determined in the liver homogenate[19] using 5,5-dithiobis-(2-nitrobenzoic acid) (Ellman's reagent) to form a yellow color, which was measured at 412 nm. The concentration of blood GSH was expressed as μmol/mL and calculated using the standard curve of dilutions of GSH ranging from 0.25 to 12 μmol/mL.

2.13. Statistical Analysis. All statistical analyses were done using GraphPad Prism v7 software (GraphPad, California). Data were expressed as mean ± SE. One-way analysis of variance (ANOVA) was carried out, followed by Tukey's multiple comparison test. A value of $p < 0.05$ was considered statistically significant. For measuring the power of statistical significance, the effect size was calculated using Cohen's effect (Cohen's d) to verify the analysis of some results.[20] The classification used was as follows: small effect (≥0.2), medium effect (≥0.50), and large effect (≥0.8).

2.14. Histopathological Examination of Heart and Aorta. Heart and aorta specimens from each group were collected and fixed in 10% neutral buffered formalin. The specimens were embedded in paraffin to be sliced into 5 μm thick sections on glass slides (positively charged) and stained by hematoxylin and eosin (H&E).

2.15. UHPLC-Orbitrap-HRMS Analysis. Qualitative identification of the secondary metabolites in the leaves and flowers was performed[12] using the UHPLC system (Dionex UltiMate 3000, Thermo Fischer Scientific) with an RP-18 column (particle size 1.8 μm, pore size 100 Å, 150 mm × 1 mm i.d., Acquity HSS T3, Waters) using water (A) and acetonitrile (B) with 0.1% formic acid as mobile phases and a photodiode array detector (220−600 nm, Thermo Fischer Scientific) for UV analysis. The binary gradient was 0−1 min (isocratic 95% A, 5% B), 1−11 min (a linear increase of B from 5 to 100%), 11−19 min (isocratic 100% B), and 19−30 min (isocratic 5% B). The flow rate was 150 μL/min, and the injection volume was 2 μL. The collision-induced dissociation (CID) mass spectra (buffer gas; helium) were done from an Orbitrap Elite mass spectrometer (Thermo Fischer Scientific, Darmstadt, Germany) provided with a heated electrospray ion source (adjusted at 3 kV in negative mode and 4 kV in positive mode with a capillary temperature of 300 °C, a source heater temperature of 250 °C, and an FTMS resolution of 30.000). Pierce ESI negative ion calibration solution (product no. 88324) and Pierce ESI positive ion calibration solution (product no. 88323) (from Thermo Fisher Scientific) were used for applying calibration. The data were processed using the software Xcalibur 2.2 SP1 (Thermo Fisher Scientific, USA).

https://doi.org/10.1021/acsomega.2c05356
ACS Omega 2022, 7, 46524−46535

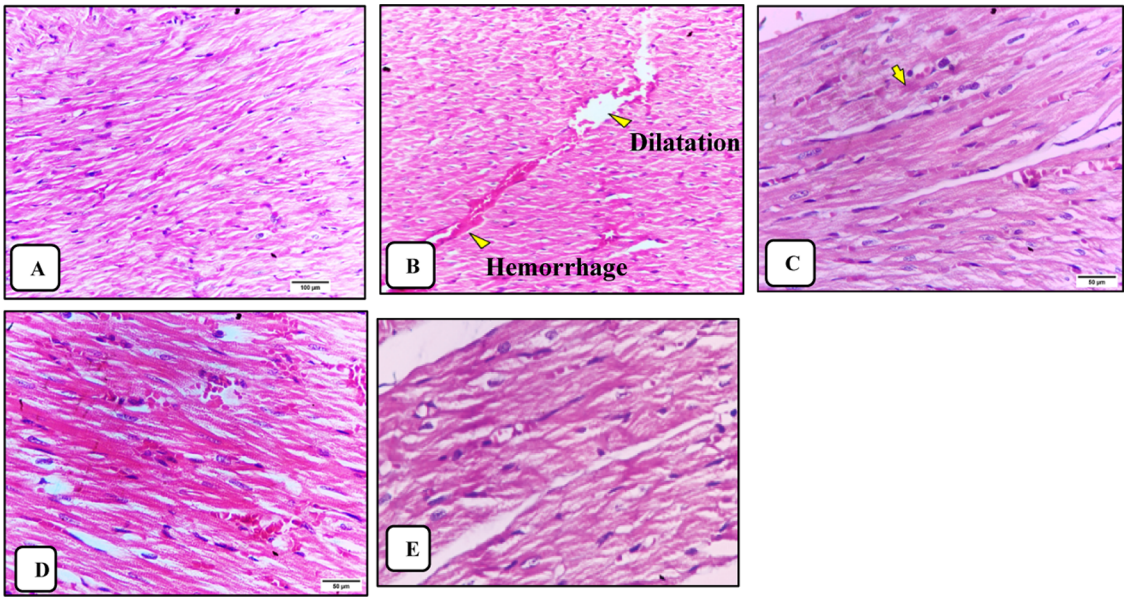

Figure 1. Photomicrographs of cross sections of heart stained with H&E in rats of normal control (×100) (A), hypertensive control (×100) (B), lisinopril (×200) (C), ethanolic extract 250 mg/kg (×200) (D), and ethanolic extract 500 mg/kg (×200) (E).

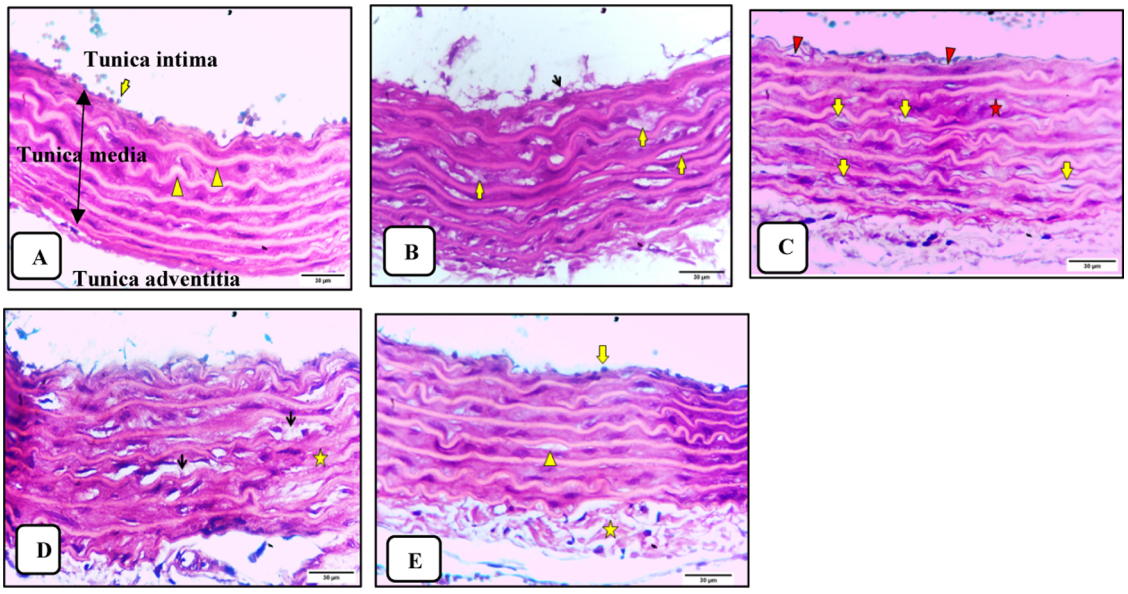

Figure 2. Photomicrographs of cross sections of aorta stained with H&E in rats (×400) of normal control (A), hypertensive control (B), lisinopril (C), ethanolic extract 250 mg/kg (D), and ethanolic extract 500 mg/kg (E).

3. RESULTS

3.1. Blood Pressure Measurements. Daily administration of the ethanolic extract of the leaves in doses 250 and 500 mg/kg significantly attenuated the elevated systolic blood pressure (120.9 ± 4.0 and 114.6 ± 6.7 mmHg, respectively) compared to L-NAME-induced hypertensive rats (Table 1).

3.2. Electrocardiography (ECG) Determination. The normal rats' ECG presented a defined RR interval, PR interval, and QRS complex with normal ranges. Daily administration of the ethanolic extract of the leaves in dose 250 mg/kg significantly decreased the PR interval, while the administration of the high dose 500 mg/kg significantly decreased the RR and the PR intervals compared to L-NAME-induced hypertensive rats (Table 2). Lisinopril and both doses of the ethanolic extract did not show significant changes in the QRS intervals.

3.3. Determination of Serum Angiotensin-Converting Enzyme (ACE) Concentration. Daily administration of lisinopril and the ethanolic extract of the leaves in dose 500 mg/kg for six weeks significantly decreased the elevated serum ACE (254.7 ± 5.1 and 261.6 ± 2.4 pg/mL, respectively) compared to L-NAME-induced hypertensive rats (288.8 ± 0.6 pg/mL) (Table 1).

3.4. Determination of Serum Nitric Oxide (NO) Concentration. The ethanolic extract of the leaves in the two doses 250 and 500 mg/kg significantly restored the decreased serum nitric oxide levels compared to L-NAME-induced hypertensive rats (Table 1).

https://doi.org/10.1021/acsomega.2c05356
ACS Omega 2022, 7, 46524−46535

Table 3. Metabolites Detected in the Methanolic Extract of *C. ignea* A[a]

peak no.	R_t (min)	UV	mode	molecular ion m/z (+/−) (ppm)	elemental composition	error (ppm)	MS/MS (+/−) (ppm)	identification	leaf	flower
1	0.59		N	181.07152	$C_6H_{13}O_6^-$	2.539	101, 163	mannitol	+	+
2	0.6		N	179.05586	$C_6H_{11}O_6^-$	−1.812	134	monosaccharide (hexose)	+	+
3	0.65		N	341.10858	$C_{12}H_{21}O_{11}^-$	−1.869	143, 161, 179, 215	disaccharide	+	+
4	0.72	253	N	191.05577	$C_7H_{11}O_6^-$	0.755	111, 173	quinic acid	+	+
5	0.88	273	N	331.06641	$C_{13}H_{15}O_{10}^-$	1.320	125, 169, 211, 271	galloyl hexoside	−	+
6	1.04	271	N	169.01402	$C_7H_5O_5^-$	0.870	125	gallic acid	+	+
7	1.52	269	N	633.07275	$C_{27}H_{21}O_{18}^-$	1.595	249, 275, 301, 463, 481	galloyl-hexahydroxydiphenoylhexoside (corilagin)	+	+
8	1.61	264, 293	N	315.07132	$C_{13}H_{15}O_9^-$	0.262	153, 109	protocatechuic acid hexoside	+	−
9	1.75		N	325.05588	$C_{14}H_{13}O_9^-$	−1.564	125, 169	galloylshikimic acid	−	+
10	1.87	268	N	483.07623	$C_{20}H_{19}O_{14}^-$	−1.452	169, 313, 331	digalloyl hexoside	−	+
11	2.09	273	N	801.07355	$C_{34}H_{25}O_{23}^-$	−5.696	757	punigluconin	+	−
12	5.11	269	N	183.02806	$C_8H_7O_5^-$	−0.740	124, 168	methyl gallate	+	+
13	8.89	271	N	783.06671	$C_{34}H_{23}O_{22}^-$	−1.071	301, 613, 633, 765	pedunculagin I	+	+
14	9.12	269, 330	P	595.16498	$C_{27}H_{31}O_{15}^+$	−1.288	271, 433	apigenin-*O*-di-hexoside	−	+
15	9.17	271, 356	N	611.15973	$C_{27}H_{31}O_{16}^-$	−1.425	287, 449	flavonoid-*O*-di-hexoside	−	+
16	9.29	269	N	367.10187	$C_{17}H_{19}O_9^-$	−1.331	134, 191, 193	feruloylquinic acid	+	−
17	9.31	269	N	483.07693	$C_{20}H_{19}O_{14}^-$	−0.003	169, 313, 331	digalloyl hexose	+	+
18	9.35		N	447.14954	$C_{19}H_{27}O_{12}^-$	−0.364	269, 285, 401	unidentified	+	−
19	9.53	298	N	387.16495	$C_{18}H_{27}O_9^-$	−0.023	163, 207, 225, 369	tuberonic acid hexoside	+	−
20	9.55	273	N	1175.60315	$C_{54}H_{95}O_{27}^-$	−2.019	463, 633, 765, 785	ellagitannin	−	+
21	9.58	269	N	785.08148	$C_{34}H_{25}O_{22}^-$	−2.189	301, 483, 615, 633, 767	digalloyl-hexahydroxydiphenoylhexoside	−	+
22	9.66	269, 353	N	449.10767	$C_{21}H_{21}O_{11}^-$	−0.374	193, 229, 269, 287, 355	ferulic acid-*O*-hexoside derivative	−	+
23	9.68	268, 345	N	431.09692	$C_{21}H_{19}O_{10}^-$	−0.819	241, 269	apigenin-*O*-hexoside	−	+
		268, 345	P	433.11206	$C_{21}H_{21}O_{10}^+$	−1.993	271	apigenin-*O*-hexoside	−	+
24	9.72	268	N	859.07111	$C_{39}H_{23}O_{23}^-$	10.135	301, 483, 613, 633, 765, 783	pedunculagin I derivative	−	+
25	9.77		N	385.18646	$C_{19}H_{29}O_8^-$	0.898	205, 223	roseoside	+	−
26	9.93	269, 369	N	627.15497	$C_{27}H_{31}O_{17}^-$	−0.966	285, 301, 345, 447, 465	kaempferol derivative	−	+
27	9.94	267, 252	N	389.18079	$C_{18}H_{29}O_9^-$	0.465	227, 329, 371	unidentified	+	−
28	9.99	269, 369	N	631.09204	$C_{28}H_{23}O_{17}^-$	−1.482	271, 317, 461, 479, 613	myricetin galloyl hexoside	+	−
29	10.13	273	P	769.08752	$C_{34}H_{25}O_{21}^+$	−0.993	303, 429, 599	unknown ellagitannin	−	+
30	10.17	265, 352	N	615.09723	$C_{28}H_{23}O_{16}^-$	− 0.099	179, 301, 463	quercetin galloyl hexoside	+	−
		264, 352	P	617.11346	$C_{28}H_{25}O_{16}^+$	−0.099	303, 315, 345, 599	quercetin galloyl hexoside	+	−
31	10.23	217, 313	N	433.11304	$C_{21}H_{21}O_{10}^-$	0.893	151, 271	naringenin-*O*-hexoside	−	+
32	10.28	264, 361	N	463.08691	$C_{21}H_{19}O_{12}^-$	−0.415	151, 179, 316, 317	myricetin-3-*O*-rhamnoside	+	+
		264, 361	P	465.10284	$C_{21}H_{21}O_{12}^+$	0.188	303, 319, 447	myricetin-3-*O*-rhamnoside	+	−
33	10.45	267, 361	N	609.14459	$C_{27}H_{29}O_{16}^-$	−0.691	179, 300, 301, 429, 447	quercetin-3-*O*-hexosyl (1 → 2) rhamnoside	+	−
34	10.47	268, 360	N	599.10260	$C_{28}H_{23}O_{15}^-$	−0.912	285, 313, 447	kaempferol galloyl hexoside	−	+
		268, 360	P	601.11920	$C_{28}H_{25}O_{15}^+$	0.404	287, 315, 349, 449, 583	kaempferol galloyl hexoside	−	+
35	10.49	265, 260	N	433.07614	$C_{20}H_{17}O_{11}^-$	−0.918	151, 179, 300, 301	quercetin-3-*O*-pentoside	+	−
36	10.50	266, 360	N	447.09213	$C_{21}H_{19}O_{11}^-$	−0.058	151, 179, 284, 285	kaempferol-3-*O*-hexoside	−	+
37	10.59	267, 363	N	447.09216	$C_{21}H_{19}O_{11}^-$	−0.062	151, 179, 301	quercetin-*O*-rhamnoside	+	−
38	10.65	271, 361	N	593.14954	$C_{27}H_{29}O_{15}^-$	−0.938	179, 284, 285, 413, 431	kaempferol-3-*O*-hexosyl (1 → 2) rhamnoside	−	+

https://doi.org/10.1021/acsomega.2c05356
ACS Omega 2022, 7, 46524−46535

Table 3. continued

peak no.	R_t (min)	UV	mode	molecular ion m/z (+/−) (ppm)	elemental composition	error (ppm)	MS/MS (+/−) (ppm)	identification	leaf	flower
39	10.72	268, 353	N	615.09772	$C_{28}H_{23}O_{16}^-$	−0.554	179, 317, 445, 463	myricetin galloyl rhamnoside	+	−
40	10.76	267, 354	N	431.09702	$C_{21}H_{19}O_{10}^-$	−0.587	151, 179, 285	kaempferol-*O*-rhamnoside	−	+
41	10.77	269, 349	N	435.12836	$C_{21}H_{23}O_{10}^-$	−0.490	273	phloretin-*O*-hexoside	+	−
42	10.79	257, 369	N	317.02957	$C_{15}H_9O_8^-$	−0.543		myricetin	+	−
		257, 369	P	319.04507	$C_{15}H_{11}O_8^+$	1.023	153, 165, 245, 263, 273, 301	myricetin	+	−
43	10.87	359	N	551.10254	$C_{24}H_{23}O_{15}^-$	−1.100	328, 343	tri-*O*-methyl ellagic acid derivative	+	+
44	11.00	271	N	643.29498	$C_{31}H_{47}O_{14}^-$	−1.052	329, 481, 595	unidentified	−	+
45	11.00	268, 354	N	599.10193	$C_{28}H_{23}O_{15}^-$	−1.112	301, 447	quercetin galloyl rhamnoside	+	−
46	11.01	269, 259	N	541.28485	$C_{24}H_{45}O_{13}^-$	−1.141	363, 495	unidentified	+	−
47	11.02	258, 367	N	301.03366	$C_{15}H_9O_7^-$	−2.056		quercetin	+	+
		258, 367	P	303.05026	$C_{15}H_{11}O_7^+$	1.092	137, 153, 165, 229, 247, 257, 275, 285	quercetin	+	+
48	11.07	358	N	537.28949	$C_{25}H_{45}O_{12}^-$	−1.979	329	di-*O*-methyl ellagic acid derivative	−	+
49	11.12	265, 340	N	271.06165	$C_{15}H_{11}O_5^-$	3.695		naringenin	−	+
		265, 340	P	273.07574	$C_{15}H_{13}O_5^+$	−0.037	147,153, 217, 245, 255	naringenin	−	+
50	11.18	268, 365	N	285.03970	$C_{15}H_9O_6^-$	1.177	151, 213, 241, 243, 257	kaempferol	+	+
		268, 365	P	287.05524	$C_{15}H_{11}O_6^+$	0.785	121, 153, 165, 213, 231, 241, 269	kaempferol	+	+
51	11.20	279, 360	N	315.05075	$C_{16}H_{11}O_7^-$	0.865		isorhamnetin	−	+
52	11.43	219	N	327.21716	$C_{18}H_{31}O_5^-$	1.710	171, 211, 229, 291, 309	trihydroxy-octadecadienoic acid ($C_{18:2}$)	+	+
53	11.58	220	N	329.23236	$C_{18}H_{33}O_5^-$	0.332	171, 211, 229, 293, 311	trihydroxy-octadecenoic acid ($C_{18:1}$)	+	+
54	11.75	220	N	287.22202	$C_{16}H_{31}O_4^-$	1.163	241, 269	dihydroxy-hexadecanoic acid ($C_{16:0}$)	+	+
55	11.83	223	N	343.04630	$C_{17}H_{11}O_8^-$	−0.127	297, 313, 328	tri-*O*-methyl ellagic acid	+	+
		223	P	345.06067	$C_{17}H_{13}O_8^+$	0.511	313, 330, 331	tri-*O*-methyl ellagic acid	+	+
56	11.87	222	P	274.27432	$C_{16}H_{36}O_2N^+$	0.197	106, 230, 256	unidentified fatty acid amide	+	−
57	11.90	220	N	309.20621	$C_{18}H_{29}O_4^-$	0.563	171, 251, 291	dihydroxy-octadecatrienoic acid ($C_{18:3}$)	+	+
58	11.95	221	N	307.19070	$C_{18}H_{27}O_4^-$	1.023	185, 235, 271, 289	hydroxy-oxo-octadecatrienoic acid ($C_{18:3}$)	+	−
59	12.38	220	N	311.22238	$C_{18}H_{31}O_4^-$	2.230	171,211, 293	dihydroxy-octadecadienoic acid ($C_{18:2}$)	+	+
60	12.41	221	N	293.21118	$C_{18}H_{29}O_3^-$	1.974	113, 185, 249, 275	hydroxy-octadecatrienoic acid ($C_{18:3}$)	−	+
61	12.80	221	N	293.21130	$C_{18}H_{29}O_3^-$	0.610	171, 195, 223, 275	hydroxy-octadecatrienoic acid ($C_{18:3}$) isomer	+	−
62	12.91	222	P	277.21619	$C_{18}H_{29}O_2^+$	−0.060	135, 149, 241, 259	unidentified fatty acid	+	−
63	13.14	222	N	295.22690	$C_{18}H_{31}O_3^-$	0.436	171, 195, 251, 277	hydroxy-octadecadienoic acid ($C_{18:2}$)	+	+
64	13.21	222	P	279.23193	$C_{18}H_{31}O_2^+$	0.262	243, 261	linolenic acid (Octadecatrienoic acid) ($C_{18:3}$)	+	+
65	13.29	224	N	471.34644	$C_{30}H_{47}O_4^-$	−0.947	423	corosolic acid	+	−
66	13.40		N	571.28693	$C_{39}H_{39}O_4^-$	4.628	241, 255, 315, 391	unidentified	+	−
67	14.40	225	N	455.35190	$C_{30}H_{47}O_3^-$	−0.158	407	ursolic acid	+	−
68	14.62	225	P	282.27933	$C_{18}H_{36}ON^+$	0.669	265, 247	octadecenoic acid amide (Oleamide)	+	+
69	14.91	225	P	609.27106	$C_{27}H_{45}O_{15}^+$	−6.954	531, 591	unidentified	+	−
70	15.06	226	P	593.27618	$C_{34}H_{41}O_9^+$	1.788	533	unidentified	+	+
71	16.31	224	P	607.29163	$C_{35}H_{43}O_9^+$	2.521	547	unidentified	+	+
72	16.71	225	P	338.34155	$C_{22}H_{44}ON^+$	−0.566	303, 321	docosenoic acid amide (docosenamide)	+	+
73	17.68	226	N	341.26883	$C_{20}H_{37}O_4^-$	0.568	269, 313	eicosanedioic acid	+	+

https://doi.org/10.1021/acsomega.2c05356
ACS Omega 2022, 7, 46524−46535

Table 3. continued

[a]DC. leaves and flowers *via* UHPLC-Orbitrap-HRMS in the negative and positive ionization modes.

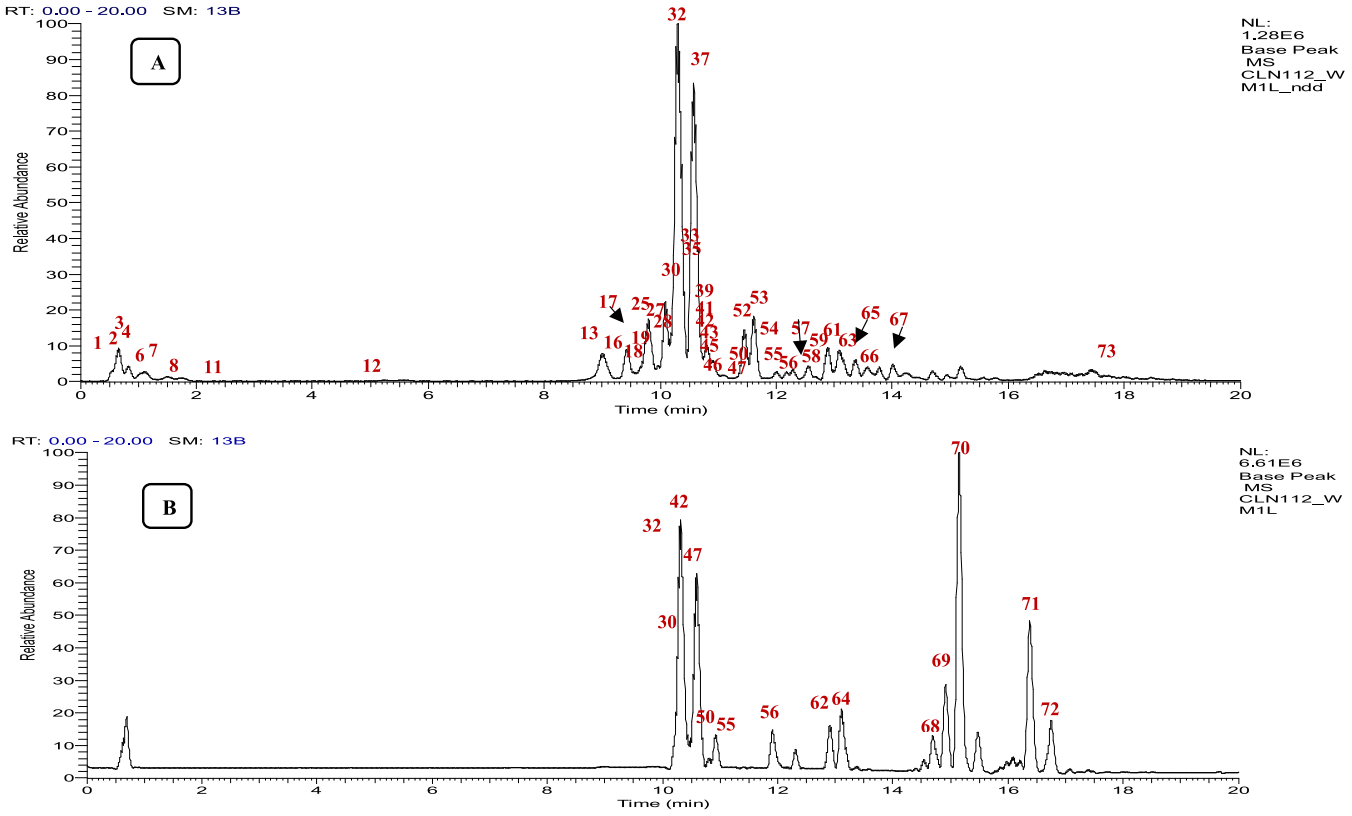

Figure 3. UHPLC-Orbitrap-HRMS total ion chromatogram (TIC) of the methanolic extract of *C. ignea* A. DC. leaves in the negative ionization mode (A) and in the positive ionization mode (B).

3.5. Determination of Malondialdehyde (MDA). The elevated MDA levels were significantly decreased by the two doses 250 and 500 mg/kg (2.2 ± 0.3 and 2.0 ± 0.2 nmol/mL, respectively) in the liver homogenate compared to L-NAME-induced hypertensive rats (3.2 ± 0.3 nmol/mL) (Table 1).

3.6. Determination of Glutathione (GSH). Lisinopril and the ethanolic extract of the leaves in the high dose 500 mg/kg significantly restored the decreased GSH levels (9.5 ± 0.4 and 9.2 ± 0.9 μmol/mL, respectively) in the liver homogenate compared to L-NAME-induced hypertensive rats (7.3 ± 0.1 μmol/mL) (Table 1).

The effect size was calculated for each dose in all tested parameters, where the two doses showed a large effect compared with the hypertensive control. The high dose (500 mg/kg) and the low dose (250 mg/kg) both showed a large effect in the blood pressure measurements (d = 2 and 1.9, respectively). For the ACE determination, effect sizes were 1.3 for the low dose and 2.7 for the high dose. In the determination of MDA, the high dose showed a larger effect size (Cohen's d = 2.1) than the low dose (d = 1.5), while in the GSH test, the lower dose showed a larger d value (4.02) compared to the high dose having the effect size (d) = 1.7. The effect size in the NO measurement was 2.2 for both doses.

3.7. Histopathological Examination of Heart and Aorta. Examination of the heart of the normal control group revealed that the heart tissues were within the normal limit, where the muscle fibers were arranged in bundles parallel to each other. Microscopic examination of heart tissues in L-NAME-induced hypertensive rats showed dilatation of blood capillaries and hemorrhage between the cardiac tissues. The cross sections of the heart of rats in the group treated with 500 mg/kg showed less degeneration in the cardiac muscle bundles with no hemorrhage observed (Figure 1).

Upon examination of the aorta (Figure 2), the normal control group showed a normal histological structure of tunica intima, tunica media (composed of arranged elastic laminae and smooth muscle cells between the elastic laminae), and tunica adventitia. L-NAME-induced hypertensive rats showed various histopathological alterations and thickening in the cross section of aorta which showed erosion of endothelial cells of tunica intima. Tunica media showed degeneration and vacuolation of smooth muscle cells between the elastic laminae. Also, degeneration and edema of tunica adventitia were observed. The cross sections of aorta of rats in the group treated with 250 mg/kg ethanolic extract of the leaves showed mild erosion of endothelial cells of tunica intima with some vacuolation of smooth muscle cells between the elastic laminae and degeneration of tunica adventitia. In the group treated with 500 mg/kg ethanolic extract of the leaves, the cross section of aorta showed reduced degenerations in the tunica media and tunica adventitia compared to the hypertensive rats.

3.8. UHPLC-Orbitrap-HRMS Analysis. The analytical method applied enabled the identification of 53 compounds tentatively. The identified compounds belonged to various classes. Assignment of metabolites was performed by comparing retention time, UV spectra, and MS data (accurate

https://doi.org/10.1021/acsomega.2c05356
ACS Omega 2022, 7, 46524−46535

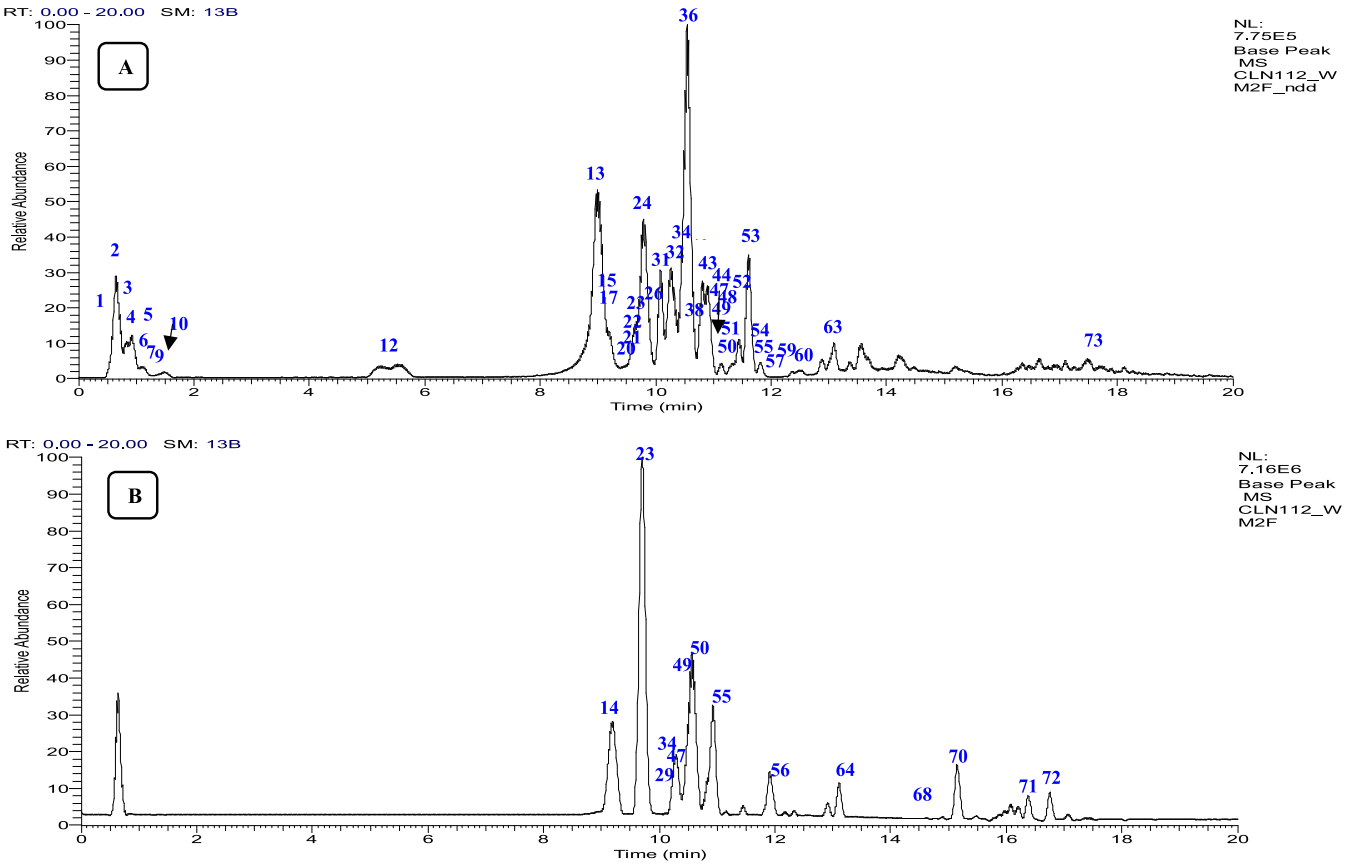

Figure 4. UHPLC-Orbitrap-HRMS total ion chromatogram (TIC) of the methanolic extract of *C. ignea* A. DC. flowers in the negative ionization mode (A) and in the positive ionization mode (B).

protonated/deprotonated mass, isotopic distribution, and fragmentation pattern in both the positive and negative ionization modes) of the detected compounds with the reported in the literature for genus *Cuphea*[8,11,21,22] in addition to using the phytochemical dictionary of the natural product database (compact reinforced composite, CRC, Wiley). The identified metabolites were assigned as seven hydrolysable tannins, one ellagic acid derivative, four hydroxybenzoic acid derivatives, two hydroxycinnamic acid derivatives, twenty-one flavonoids, two triterpenoid acids, thirteen fatty acids, and three miscellaneous compounds. A total of 47 metabolites were identified for the first time in the plant (Table 3). Thirty-eight and thirty-five compounds were identified in the leaves and flowers, respectively (Figures 3 and 4).

3.8.1. Hydrolysable Tannins. Hydrolysable tannins have a central part of a β-glucopyranosyl group attached to galloyl groups (gallotannins) or ellagitannins.[8] Hydrolysable tannins were only detected in the negative ionization mode. Gallotannins composed of monomeric and dimeric galloyl parts linked to a hexose sugar were also detected. Two gallotannins were identified in the flowers, where they showed nearly identical UV spectra similar to those of gallic acid (λ_{max} = 269 nm).[23,24] Peak 5 showed a base peak at m/z 169 [M-162-H]$^-$, m/z 271, and m/z 211 for the removal of two or four formaldehyde groups (CH_2O) from the hexose moiety, and it was identified as galloyl hexoside.[25]

Ellagitannins are complex structures of different numbers of galloyl and hexahydroxydiphenoyl (HHDP) units esterified with glucose. Five ellagitannins were detected in *C. ignea* A. DC. in the negative ionization mode. They were characterized by their fragment ion spectra due to the loss of galloyl (152 amu), gallate (170 amu), HHDP residue (302 amu), HHDP glucose (482 amu), galloylglucose (332 amu), and galloyl-HHDP-glucose (634 amu) residues.[24] A characteristic feature of ellagitannins is the ability to release ellagic acid (bislactone), which is formed from the hydrolytic release of HHDP ester groups, which undergo rapid, facile, and unavoidable lactonization.[26]

Peak 7 with fragment ion at m/z 481, indicating the loss of the galloyl moiety and fragment ions m/z 463 and m/z 301, indicating the ellagic acid residue, was identified as galloyl-hexahydroxydiphenoylhexoside (Corilagin).[8]

Peak 13 with [M − H]$^-$ at m/z 783.0667 and fragment ions at m/z 765 [M-18-H]$^-$, 613 [M-170-H]$^-$, and 301 [M-482-H]$^-$, indicating an ellagic acid residue, was identified as pedunculagin I (bis-HHDP-hexoside). Peak 11 was tentatively identified as punigluconin from its molecular formula ($C_{34}H_{25}O_{23}^-$), and the base peak at m/z 757 indicates the loss of a CO_2 moiety. Peak 20 was identified as ellagitannin due to the presence of the base peak at m/z 785, indicating the characteristic digalloyl-HHDP-hexoside moiety and fragment ion at m/z 633 (loss of the galloyl moiety).[27]

3.8.2. Flavonoids. The identification was based on their molecular ions, derived chemical formula, and MS fragments in addition to photodiode array (PDA) detection. Flavonols, flavones, and flavanones identified were generally glycosylated with one or more sugar units. The nature of sugars could be deduced from the elimination of the sugar residues in MS/MS analysis i.e., loss of 162 amu (hexose), 146 amu (deoxyhexose), and 132 amu (pentose) in *O*-glycosides. Some flavonoid

https://doi.org/10.1021/acsomega.2c05356
ACS Omega 2022, 7, 46524−46535

glycosides showed the loss of a galloyl unit (152 amu).[28] The UV maximum absorbance of flavonols was detected near 220−270 nm and a second maximum absorbance near 350−370 nm.

Flavonols: The MS/MS analysis in the positive ionization mode revealed the identification of flavonol aglycones; quercetin, kaempferol, and myricetin generally exhibited dehydration, loss of CO, and breakage of the C-ring. Loss of H_2O and CO can be observed from the molecular ion and its fragments. The cleavage at ring C follows the retro Diels−Alder (RDA) arrangement, and the produced fragments give an indication to the substitution of the A- and B-rings.[29]

Quercetin, kaempferol, and myricetin glycosides were the abundant constituents identified with diagnostic mass fragments obtained in the negative mode at 301, 285, and 317, respectively.[28] The formation of flavonol aglycone radical ions $[Y_0\text{-H}]^-$. in a high abundance compared to the aglycone ion $[Y_0]^-$ is correlated with the glycosylation at the 3-*O* position, which was reported in peaks 32, 35, 36, 33 and 38.[30] The ESI-MS spectra of peak 47 in the positive ionization mode with $[M + H]^+$ at *m*/*z* 303.05026 were assigned to *quercetin*,[29] those of peak 42 with $[M + H]^+$ at *m*/*z* 319.045.7 were confirmed as myricetin,[29] and those of peak 51 were tentatively identified as isorhamnetin from its molecular ion at *m*/*z* 315.05075.[31]

Five flavonol-O-galloyl glycosides were identified in the leaves and flowers of *C. ignea* A. DC. mainly in the negative ionization mode. They all show the characteristic loss of 152 amu for the galloyl moiety in peaks 30, 34, 45, 39, and 28. Peak 30 demonstrated the loss of galloyl part $[M\text{-}152\text{-}H]^-$ by the base peak at *m*/*z* 463 and a product ion at *m*/*z* 301 and so identified as *quercetin galloyl hexoside*. Peaks 34 and 45 demonstrated the loss of the galloyl moiety by the product ion at *m*/*z* 447, and they showed another fragment ion at *m*/*z* 285 and 301, respectively, and were confirmed to be kaempferol galloyl hexoside and quercetin galloyl rhamnoside, respectively.[32]

Quercetin-*O*-monoglycosides were represented by peaks 35 and 37.[33] Kaempferol-*O*-monoglycosides were detected in the flowers in peaks 36 and 40 identified as kaempferol-3-*O*-hexoside and kaempferol-*O*-rhamnoside, respectively.[34] Myricetin-*O*-glycoside was represented by peak 32.

Flavonol-*O*-diglycosides were detected at peaks 33 and 38. Peak 33 showed a base peak at *m*/*z* 300 $[M\text{-}162\text{-}146\text{-}2H]^-$, indicating quercetin aglycone with hexosyl rhamnoside residue at the 3-*O* position. Fragment ions at *m*/*z* 447 $[M\text{-}162\text{-}H]^-$ in addition to the abundant fragment ion at *m*/*z* 429 $[M\text{-}162\text{-}18\text{-}H]^-$ referred to the loss of terminal hexosyl residue, followed by the loss of water molecules and suggested the (1 → 2) glycosidic linkage; therefore, it was assigned as quercetin-3-O-hexosyl (1 → 2) rhamnoside. Similarly, peak 38 was assigned as kaempferol-3-*O*-hexosyl (1 → 2) rhamnoside.[30,35,36]

Flavones, flavanones, and dihydrochalcone derivatives: Two flavone derivatives were detected in the flowers of *C. ignea* A. DC. represented by peaks 23 and 14. Peak 23 was detected in both ionization modes identified as apigenin-*O*-hexoside.[31] Peak 49 with $[M + H]^+$ at *m*/*z* 273.07574 was identified as naringenin and its *O*-monoglycoside was detected in peak 31 identified as naringenin-*O*-hexoside.[29] Peak 41 showed a base peak at *m*/*z* 273 for phloretin aglycone and so assigned as phloretin-*O*-hexoside.[37]

3.8.3. Hydroxybenzoic Acid Derivatives. Peak 6 was identified as gallic acid, showing UV maximum at 271 nm with $[M - H]^-$ at *m*/*z* 169.014.[38] Similarly, peak 9 yielded a base peak at *m*/*z* 169 $[M\text{-}156\text{-}H]^-$ (loss of shikimic acid) and identified as galloylshikimic acid.[25] Peak 12 with fragment ions at *m*/*z* 168 due to the loss of a methyl residue and *m*/*z* 124 $[M\text{-}15\text{−}44\text{-}H]^-$ identified as methyl gallate.[39] Peak 8 showed a base peak at *m*/*z* 153 $[M\text{-}162\text{-}H]^-$ and fragment ions at *m*/*z* 109 $[M\text{-}162\text{-}44\text{-}H]^-$ and was identified as protocatechuic acid hexoside.[40] Gallic acid and methyl gallate were previously reported in *C. ignea* A. DC.[11]

3.8.4. Ellagic Acid Derivative. Peak 55 showed a $[M - H]^-$ ion at *m*/*z* 343.0463, which produced ions at *m*/*z* 328 $[M\text{-}CH_3\text{-}H]^-$, *m*/*z* 313 $[M\text{-}2CH_3\text{-}H]^-$ and *m*/*z* 298 $[M\text{-}3CH_3\text{-}H]^-$. This fragmentation pattern agreed with tri-*O*-methyl ellagic acid.[32]

3.8.5. Hydroxycinnamic Acid Derivatives. Two hydroxycinnamic acid derivatives were detected, including peak 4 with a base peak at *m*/*z* 111 $[M\text{-}44\text{-}36\text{-}H]^-$, indicating the loss of CO_2 and 2 H_2O molecules. This fragmentation led to the identification of quinic acid.[33] Peak 16 showed a base peak at *m*/*z* 193, indicating a feruloyl moiety with a fragment ion at *m*/*z* 191 derived from the quinic acid, and the compound was identified as feruloylquinic acid.[40]

3.8.6. Fatty Acids. Thirteen fatty acids were identified, including one saturated fatty acid, one unsaturated fatty acid, nine hydroxylated fatty acids, and two fatty acid amides. The saturated fatty acid was represented by **peak 73** as eicosanedioic acid.[41] The unsaturated fatty acid was identified as linolenic acid in the positive ionization mode (peak 64).[42]

Additionally, several hydroxylated fatty acids were represented by peaks 52−54, 57−61, and 63. Mono-, di-, and trihydroxy fatty acids were identified from their detected masses, molecular formulae, and loss of water molecules, where peaks 52 and 53 identified as trihydroxy-octadecadienoic acid and trihydroxy-octadecenoic acid, respectively.[43] A dihydroxy saturated fatty acid was identified as dihydroxy-hexadecanoic acid (peak 54).[41] Peaks 60 and 63 showed patterns for hydroxy unsaturated fatty acids identified as hydroxy-octadecatrienoic acid and hydroxy-octadecadienoic acid, respectively.[43] Peak 58 was identified as hydroxy-oxo-octadecatrienoic acid.[41]

Two fatty acid amides were identified in the positive ionization mode from their even masses for peaks 68 and 72 at *m*/*z* 282.27933 and *m*/*z* 338.34155 and were identified as octadecenoic acid amide (oleamide) and docosenoic acid amide (docosenamide), respectively.[42] Fatty acid amides were not identified before in genus *Cuphea*.

3.8.7. Triterpenoids. Two triterpene acids were identified in the leaves (peak 65 and 67) with similar fragmentation patterns and molecular formulae assigned for pentacyclic triterpene structures. Both compounds showed base peaks at *m*/*z* 423 and *m*/*z* 407, respectively, due to the loss of HCHO and H_2O fragments, which were matched with the fragmentation pattern of corosolic acid and ursolic acid.[44,45] Corosolic acid was identified for the first time in genus *Cuphea*.

3.8.8. Miscellaneous Compounds. Peak 19 showed a $[M - H]^-$ ion at *m*/*z* 387.1649 with fragments at *m*/*z* 369 $[M\text{-}H_2O\text{-}H]^-$. This data was previously reported for tuberonic acid hexoside (12-hydroxyjasmonic acid hexoside) in *C. carthagenensis* (Jacq.) J.F.Macbr.[8] Peak 25 represented the formate adduct form of roseoside ($C_{19}H_{29}O_8^-$) with a base peak at *m*/*z* 385.18646.[46,47] Peak 1 was identified as mannitol, which was detected before in *Cuphea hyssopifolia* and *Cuphea wrightii*.[21,22]

4. DISCUSSION

The *in vivo* study of the effect of the ethanolic extract of *C. ignea* A. DC. leaves on L-NAME-induced hypertensive rats

https://doi.org/10.1021/acsomega.2c05356
ACS Omega 2022, 7, 46524−46535

compared to lisinopril was studied for the first time in genus *Cuphea*. In the search for natural antihypertensive drugs, L-NAME has been used in many research models as a standard method for induction of hypertension.[48,49] It acts by inhibiting nitric oxide synthase, which decreases NO production, resulting in an increase in ACE concentration in serum and consequently increasing blood pressure. Decreasing ACE levels and increasing NO in serum represent a valid indicator of an active antihypertensive agent, especially if it is from a natural source, which can aid in controlling hypertension with less side effects and considerable safety compared to the widely used synthetic antihypertensive agents *e.g.*, captopril.[50]

The current study revealed that the ethanolic extract of the leaves in both doses significantly normalized the elevated systolic blood pressure, where the high dose (500 mg/kg) also possessed lowering of ACE levels in serum. These results clearly support the *in vitro* antihypertensive activity previously reported by the authors for the ethanolic extract of the leaves.[9] Also, recent studies on other *Cuphea* species *viz.*, *Cuphea glutinosa* and *C. carthagenesis* revealed significant *in vitro* ACE inhibition for both plant extracts, in addition to high kaempferol, quercetin, and myricetin glycoside content previously reported for their ACE inhibition activities.[50] Restored nitric oxide levels exhibited by the ethanolic extract in both dose levels participated to a large extent in the blood pressure-lowering activity *via* vasorelaxation effect as reported for *C. carthagenesis* Jacq McBride on aortic rings.[51]

Regarding the oxidative stress parameters, both doses displayed a significant reduction in lipid peroxidation (MDA level) and the high dose significantly restored the GSH level. The antioxidant activity of the ethanolic extract demonstrated in this study in addition to *in vitro* antioxidant activity previously reported[9] plays a key important role in managing hypertension by increasing nitric oxide bioavailability. *C. ignea* A.C. leaf extract was previously tested for its antioxidant effect in the same doses used in the current study (250 and 500 mg/kg), and the results reported an increase in GSH with reduction in MDA levels in rats in agreement with our results. The ethanolic extract at 250 mg/kg increased GSH by 65.24% and decreased MDA by 41.1% tested in the gastric homogenate of rats after induction of gastric ulcer.[52]

The results also indicate that the lower dose of the extract (250 mg/kg) could significantly lower the systolic blood pressure and restore NO levels nearly to the normal blood levels, together with a reduction in MDA and ACE. This gives the extract a great privilege as a natural candidate for antihypertensive targeted formulations and adjuvant therapies. The effect size calculation for the two doses compared to the hypertensive control showed a large effect for both doses in all of the tested parameters.

Despite all of these findings, some limitations ought to be noted in this study. First, using only five rats in each group may not be sufficient to validate and generalize the results. The larger the number of rats in each group, the results will be more significantly related to the population. Second, the study depended on measuring several parameters as an indication of hypertension, while other parameters should have been measured to assure the results and study the mechanism in more detail, including, for example, measuring the heart rate, diastolic blood pressure, serum cardiac troponin T, serum angiotensin 1−7, and superoxide dismutase.

The UHPLC-Orbitrap-HRMS study is considered the first detailed metabolic profile for leaves and flowers of *C. ignea* A. DC. The analysis led to the identification of 53 compounds, including seven hydrolysable tannins, one ellagic acid derivative, four hydroxybenzoic acid derivatives, two hydroxycinnamic acid derivatives, twenty-one flavonoids, two triterpenoid acids, thirteen fatty acids, and three miscellaneous compounds.

Regarding flavonoids, quercetin, kaempferol, and myricetin glycosides were considered the major constituents identified. These flavonol glycosides were reported to exhibit antihypertensive effects through inhibiting ACE *via in vitro* experiments or *in silico* studies due to the similar interaction with ACE active sites when compared to the well-known synthetic ACE inhibitory drugs, *e.g.*, captopril and lisinopril.[53]

Several identified compounds were also reported to have antihypertensive properties *via* ACE inhibition as quercetin, quercetin-3-*O*-rhamnoside, kaempferol, gallic acid, and methyl gallate.[53−55] Corilagin was reported to exert antihypertensive activity in hypertensive rats.[56] Additionally, hydrolysable tannins are known to possess antihypertensive action.[57] These reports support the contribution of the identified compounds to the antihypertensive activity of the plant.

5. CONCLUSIONS

In our search for a natural antihypertensive agent used for the management of hypertension and related heart disorders, the current *in vivo* antihypertensive study provided clear evidence for the activity and confirmed previous *in vitro* ACE and renin inhibition assay results on *C. ignea* A. DC. The *in vivo* study suggested several complimentary mechanisms for the *C. ignea* A. DC. ethanolic extract in management of hypertension, including ACE reduction, increased nitric oxide bioavailability, and antioxidant characteristics. A UHPLC-Orbitrap-HRMS study revealed the metabolite profile of the plant with several identified metabolites previously reported for having antihypertensive properties. Herein, this study established clear evidence for the use of *C. ignea* A. DC. as a complementary treatment in the management of hypertension, introducing a new member to natural drugs used in hypertension. Further biological studies and clinical trials should be carried out to further support the obtained results and allow its use as a natural antihypertensive agent.

AUTHOR INFORMATION

Corresponding Author

Walaa M. Ismail − *Department of Pharmacognosy, Faculty of Pharmacy, Cairo University, Cairo 11562, Egypt;* orcid.org/0000-0001-5205-8405; Phone: +201155521100; Email: walaa.ismail@pharma.cu.edu.eg

Authors

Shahira M. Ezzat − *Department of Pharmacognosy, Faculty of Pharmacy, Cairo University, Cairo 11562, Egypt; Department of Pharmacognosy, Faculty of Pharmacy, October University for Modern Sciences and Arts (MSA), Giza 12451, Egypt;* orcid.org/0000-0003-2232-7357

Aliaa E.M.K. El-Mosallamy − *Department of Pharmacology, National Research Centre, 12622 Giza, Egypt*

Kadriya S. El Deeb − *Department of Pharmacognosy, Faculty of Pharmacy, Cairo University, Cairo 11562, Egypt*

Ahlam M. El-Fishawy − *Department of Pharmacognosy, Faculty of Pharmacy, Cairo University, Cairo 11562, Egypt*

Complete contact information is available at:

https://doi.org/10.1021/acsomega.2c05356
ACS Omega 2022, 7, 46524−46535

https://pubs.acs.org/10.1021/acsomega.2c05356

Notes

The authors declare no competing financial interest.

■ ACKNOWLEDGMENTS

The authors are thankful and grateful to Prof. Dr. Mohamed A. Farag, Professor at the Faculty of Pharmacy, Cairo University (Professor of Food Chemistry, American University in Cairo), for performing the analysis of the extracts using UHPLC-Orbitrap-HRMS and for his unlimited support and Ass. Prof. Dr. Rehab F. Abdel-Rahman, Pharmacology Department, National Research Centre, Giza, Egypt, for her help in the statistical analysis of the biological study.

■ REFERENCES

(1) Oparil, S.; Zaman, M. A.; Calhoun, D. A. Pathogenesis of hypertension. *Ann. Intern. Med.* **2003**, *139*, 761−776.
(2) Abdel-Rahman, R. F.; Hessin, A. F.; Abdelbaset, M.; Ogaly, H. A.; Abd-Elsalam, R. M.; Hassan, S. M. Antihypertensive Effects of Roselle-Olive Combination in L-NAME-Induced Hypertensive Rats. *Oxid. Med. Cell. Longevity* **2017**, *2017*, No. 9460653.
(3) Sparks, M. A.; Crowley, S. D.; Gurley, S. B.; Mirotsou, M.; Coffman, T. M. Classical renin-angiotensin system in kidney physiology. *Compr. Physiol.* **2011**, *4*, 1201−1228.
(4) Griendling, K. K.; Minieri, C. A.; Ollerenshaw, J. D.; Alexander, R. W. Angiotensin II stimulates NADH and NADPH oxidase activity in cultured vascular smooth muscle cells. *Circ. Res.* **1994**, *74*, 1141−1148.
(5) Krepsky, P. B.; Isidório, R. G.; De Souza Filho, J. D.; Côrtes, S. F.; Braga, F. C. Chemical composition and vasodilatation induced by *Cuphea carthagenensis* preparations. *Phytomedicine* **2012**, *19*, 953−957.
(6) Zago, A. M.; Carvalho, F. B.; Gutierres, J. M.; Bohnert, C.; Fernandes, M. d. C.; Morandini, L. M.; Coelho, H. S.; Fogaça, A. O.; Andrade, C. M.; Mostardeiro, M. A.; Dalcol, I. I.; Morel, A. F. A phytochemical study of the *Cuphea glutinosa* from Southern Brazil: Na +,K+-ATPase activity inhibition and antioxidant properties. *Nat. Prod. Res.* **2019**, *33*, 3426−3431.
(7) Anwar, M. A.; Al Disi, S. S.; Eid, A. H. Anti-hypertensive herbs and their mechanisms of action: Part II. *Front. Pharmacol.* **2016**, *7*, 50.
(8) Schaedler, M. I.; Palozi, R. A. C.; Tirloni, C. A. S.; Silva, A. O.; Araújo, V. d. O.; Lourenço, E. L. B.; de Souza, L. M.; Lívero, F. A. d. R.; Gasparotto Junior, A. Redox regulation and NO/cGMP plus K +channel activation contributes to cardiorenal protection induced by *Cuphea carthagenensis* (Jacq.) J.F. Macbr. in ovariectomized hypertensive rats. *Phytomedicine* **2018**, *51*, 7−19.
(9) Ismail, W. M.; Ezzat, S. M.; Michel, H. E.; El Deeb, K. S.; El-Fishawy, A. M. Angiotensin-converting enzyme and renin inhibition activities, antioxidant properties, phenolic and flavonoid contents of *Cuphea ignea* A. DC. *J. Rep. Pharm. Sci.* **2020**, *9*, 92.
(10) Mahmoud, D. B.; Ismail, W. M.; Moatasim, Y.; Kutkat, O.; ElMeshad, A. N.; Ezzat, S. M.; El Deeb, K. S.; El-Fishawy, A. M.; Gomaa, M. R.; Kandeil, A.; et al. Delineating a potent antiviral activity of *Cuphea ignea* extract loaded nano-formulation against SARS-CoV-2: In silico and in vitro studies. *J. Drug Delivery Sci. Technol.* **2021**, *66*, No. 102845.
(11) Hassan, S. K.; Mousa, A. M.; El-Sammad, N. M.; Abdel-Halim, A. H.; Khalil, W. K.; Elsayed, E. A.; Anwar, N.; Linscheid, M. W.; Moustafa, E. S.; Hashim, A. N.; Nawwar, M. Antitumor activity of *Cuphea ignea* extract against benzo (a) pyrene-induced lung tumorigenesis in Swiss Albino mice. *Toxicol. Rep.* **2019**, *6*, 1071−1085.
(12) Farag, M.; Ali, S.; Hodaya, R.; El-Seedi, H.; Sultani, H.; Laub, A.; Eissa, T.; Abou-Zaid, F.; Wessjohann, L. Phytochemical profiles and antimicrobial activities of *Allium cepa* red cv. and *A. sativum* subjected to different drying methods: a comparative MS-based metabolomics. *Molecules* **2017**, *22*, 761.
(13) OECD. Test No. 425, *Acute Oral Toxicity: Up-and-Down Procedure* 2008.
(14) Irvine, R. J.; White, J.; Chan, R. The influence of restraint on blood pressure in the rat. *J. Pharmacol. Toxicol. Methods* **1997**, *38*, 157−162.
(15) Cher, C. D. N.; Armugam, A.; Zhu, Y. Z.; Jeyaseelan, K. Molecular basis of cardiotoxicity upon cobra envenomation. *Cell. Mol. Life Sci. CMLS* **2005**, *62*, 105−118.
(16) Bryan, N. S.; Grisham, M. B. Methods to detect nitric oxide and its metabolites in biological samples. *Free Radical Biol. Med.* **2007**, *43*, 645−657.
(17) Miranda, K. M.; Espey, M. G.; Wink, D. A. A rapid, simple spectrophotometric method for simultaneous detection of nitrate and nitrite. *Nitric Oxide* **2001**, *5*, 62−71.
(18) Uchiyama, M.; Mihara, M. Determination of malonaldehyde precursor in tissues by thiobarbituric acid test. *Anal. Biochem.* **1978**, *86*, 271−278.
(19) Bulaj, G.; Kortemme, T.; Goldenberg, D. P. Ionization−reactivity relationships for cysteine thiols in polypeptides. *Biochemistry* **1998**, *37*, 8965−8972.
(20) Cohen, J. Statistical power analysis. *Curr. Dir. Psychol. Sci.* **1992**, *1*, 98−101.
(21) Morales-Serna, J. A.; García-Ríos, E.; Madrigal, D.; Cárdenas, J.; Salmón, M. Constituents of organic extracts of Cuphea hyssopifolia. *J. Mex. Chem. Soc.* **2011**, *55*, 62−64.
(22) Perez-Castorena, A. L.; Maldonado, E. Triterpenes and flavonoid glycosides from Cuphea wrightii. *Biochem. Syst. Ecol.* **2003**, *31*, 331−334.
(23) Fischer, U. A.; Carle, R.; Kammerer, D. R. Identification and quantification of phenolic compounds from pomegranate (*Punica granatum* L.) peel, mesocarp, aril and differently produced juices by HPLC-DAD−ESI/MSn. *Food Chem.* **2011**, *127*, 807−821.
(24) Zhu, M.; Dong, X.; Guo, M. Phenolic profiling of Duchesnea indica combining macroporous resin chromatography (MRC) with HPLC-ESI-MS/MS and ESI-IT-MS. *Molecules* **2015**, *20*, 22463−22475.
(25) Wyrepkowski, C.; Gomes da Costa, D.; Sinhorin, A.; Vilegas, W.; De Grandis, R.; Resende, F.; Varanda, E.; dos Santos, L. Characterization and quantification of the compounds of the ethanolic extract from *Caesalpinia ferrea* stem bark and evaluation of their mutagenic activity. *Molecules* **2014**, *19*, 16039−16057.
(26) Seeram, N. P.; Lee, R.; Scheuller, H. S.; Heber, D. Identification of phenolic compounds in strawberries by liquid chromatography electrospray ionization mass spectroscopy. *Food Chem.* **2006**, *97*, 1−11.
(27) Sentandreu, E.; Cerdán-Calero, M.; Sendra, J. M. Phenolic profile characterization of pomegranate (*Punica granatum*) juice by high-performance liquid chromatography with diode array detection coupled to an electrospray ion trap mass analyzer. *J. Food Compost. Anal.* **2013**, *30*, 32−40.
(28) Cuyckens, F.; Claeys, M. Mass spectrometry in the structural analysis of flavonoids. *J. Mass Spectrom.* **2004**, *39*, 1−15.
(29) Tsimogiannis, D.; Samiotaki, M.; Panayotou, G.; Oreopoulou, V. Characterization of flavonoid subgroups and hydroxy substitution by HPLC-MS/MS. *Molecules* **2007**, *12*, 593−606.
(30) Ablajan, K.; Abliz, Z.; Shang, X. Y.; He, J. M.; Zhang, R. P.; Shi, J. G. Structural characterization of flavonol 3, 7-di-O-glycosides and determination of the glycosylation position by using negative ion electrospray ionization tandem mass spectrometry. *J. Mass Spectrom.* **2006**, *41*, 352−360.
(31) Ezzat, S. M.; Raslan, M.; Salama, M. M.; Menze, E. T.; El Hawary, S. S. *In vivo* anti-inflammatory activity and UPLC-MS/MS profiling of the peels and pulps of *Cucumis melo* var. cantalupensis and *Cucumis melo* var. reticulatus. *J. Ethnopharmacol.* **2019**, *237*, 245−254.
(32) Saber, F. R.; Abdelbary, G. A.; Salama, M. M.; Saleh, D. O.; Fathy, M. M.; Soliman, F. M. UPLC/QTOF/MS profiling of two *Psidium* species and the in-vivo hepatoprotective activity of their nano-formulated liposomes. *Food Res. Int.* **2018**, *105*, 1029−1038.

https://doi.org/10.1021/acsomega.2c05356
ACS Omega 2022, 7, 46524−46535

(33) Saldanha, L.; Vilegas, W.; Dokkedal, A. Characterization of flavonoids and phenolic acids in Myrcia bella cambess. Using FIA-ESI-IT-MSn and HPLC-PAD-ESI-IT-MS combined with NMR. *Molecules* **2013**, *18*, 8402−8416.
(34) Farag, M. A.; Sharaf Eldin, M. G.; Kassem, H.; Abou el Fetouh, M. Metabolome classification of *Brassica napus* L. organs via UPLC−QTOF−PDA−MS and their anti-oxidant potential. *Phytochem. Anal.* **2013**, *24*, 277−287.
(35) Ding, S.; Dudley, E.; Plummer, S.; Tang, J.; Newton, R.; Brenton, A. Fingerprint profile of Ginkgo biloba nutritional supplements by LC/ESI-MS/MS. *Phytochemistry* **2008**, *69*, 1555−1564.
(36) Sakna, S. T.; Mocan, A.; Sultani, H. N.; El-fiky, N. M.; Wessjohann, L. A.; Farag, M. A. Metabolites profiling of *Ziziphus* leaf taxa via UHPLC/PDA/ESI-MS in relation to their biological activities. *Food Chem.* **2019**, *293*, 233−246.
(37) Mena, P.; Calani, L.; Dall'Asta, C.; Galaverna, G.; García-Viguera, C.; Bruni, R.; Crozier, A.; Del Rio, D. Rapid and comprehensive evaluation of (poly) phenolic compounds in pomegranate (*Punica granatum* L.) juice by UHPLC-MSn. *Molecules* **2012**, *17*, 14821−14840.
(38) Yang, B.; Kortesniemi, M.; Liu, P.; Karonen, M.; Salminen, J.-P. Analysis of hydrolyzable tannins and other phenolic compounds in emblic leafflower (*Phyllanthus emblica* L.) fruits by high performance liquid chromatography−electrospray ionization mass spectrometry. *J. Agric. Food Chem.* **2012**, *60*, 8672−8683.
(39) Kumar, S.; Chandra, P.; Bajpai, V.; Singh, A.; Srivastava, M.; Mishra, D.; Kumar, B. Rapid qualitative and quantitative analysis of bioactive compounds from Phyllanthus amarus using LC/MS/MS techniques. *Ind. Crops Prod.* **2015**, *69*, 143−152.
(40) Fang, N.; Yu, S.; Prior, R. L. LC/MS/MS characterization of phenolic constituents in dried plums. *J. Agric. Food Chem.* **2002**, *50*, 3579−3585.
(41) Hashem, M. M.; Salama, M. M.; Mohammed, F. F.; Tohamy, A. F.; El Deeb, K. S. Metabolic profile and hepatoprotective effect of *Aeschynomene elaphroxylon* (Guill. & Perr.). *PLoS One* **2019**, *14*, No. e0210576.
(42) Farag, M. A.; Otify, A.; Porzel, A.; Michel, C. G.; Elsayed, A.; Wessjohann, L. A. Comparative metabolite profiling and fingerprinting of genus *Passiflora* leaves using a multiplex approach of UPLC-MS and NMR analyzed by chemometric tools. *Anal. Bioanal. Chem.* **2016**, *408*, 3125−3143.
(43) Otify, A.; George, C.; Elsayed, A.; Farag, M. A. Mechanistic evidence of *Passiflora edulis* (Passifloraceae) anxiolytic activity in relation to its metabolite fingerprint as revealed via LC-MS and chemometrics. *Food Funct.* **2015**, *6*, 3807−3817.
(44) Cao, J.; Peng, L.-Q.; Xu, J.-J. Microcrystalline cellulose based matrix solid phase dispersion microextration for isomeric triterpenoid acids in loquat leaves by ultrahigh-performance liquid chromatography and quadrupole time-of-flight mass spectrometry. *J. Chromatogr. A* **2016**, *1472*, 16−26.
(45) Sut, S.; Poloniato, G.; Malagoli, M.; Dall'Acqua, S. Fragmentation of the main triterpene acids of apple by LC-APCI-MSn. *J. Mass Spectrom.* **2018**, *53*, 882−892.
(46) Spínola, V.; Pinto, J.; Castilho, P. C. Identification and quantification of phenolic compounds of selected fruits from Madeira Island by HPLC-DAD−ESI-MSn and screening for their antioxidant activity. *Food Chem.* **2015**, *173*, 14−30.
(47) Sun, Q.; Zhu, J.; Cao, F.; Chen, F. Anti-inflammatory properties of extracts from *Chimonanthus nitens* Oliv. leaf. *PLoS One* **2017**, *12*, No. e0181094.
(48) Aekthammarat, D.; Pannangpetch, P.; Tangsucharit, P. Moringa oleifera leaf extract lowers high blood pressure by alleviating vascular dysfunction and decreasing oxidative stress in L-NAME hypertensive rats. *Phytomedicine* **2019**, *54*, 9−16.
(49) Oyagbemi, A. A.; Omobowale, T. O.; Adejumobi, O. A.; Owolabi, A. M.; Ogunpolu, B. S.; Falayi, O. O.; Hassan, F. O.; Ogunmiluyi, I. O.; Asenuga, E. R.; Ola-Davies, O. E.; et al. Antihypertensive power of Naringenin is mediated via attenuation of mineralocorticoid receptor (MCR)/angiotensin converting enzyme (ACE)/kidney injury molecule (Kim-1) signaling pathway. *Eur. J. Pharmacol.* **2020**, *880*, No. 173142.
(50) Santos, M. C.; Soares, K. D.; Beltrame, B. M.; Toson, N. S.; do Carmo, B.; Pimentel, M.; Bordignon, S. A.; Apel, M. A.; Mendez, A. S.; Henriques, A. T. Polyphenolic Composition and in Vitro Antihypertensive and Anti-Inflammatory Effects of *Cuphea lindmaniana* and *Cuphea urbaniana*. *Chem. Biodivers.* **2021**, *18*, No. e2100041.
(51) Schuldt, E. Z.; Ckless, K.; Simas, M. E.; Farias, M. R.; Ribeiro-Do-Valle, R. M. Butanolic fraction from *Cuphea carthagenensis* Jacq McBride relaxes rat thoracic aorta through endothelium-dependent and endothelium-independent mechanisms. *J. Cardiovasc. Pharmacol.* **2000**, *35*, 234−239.
(52) Elgindi, M.; Ayoub, N.; Milad, R.; Mekky, R. Antioxidant and Cytotoxic Activities of *Cuphea hyssopifolia* Kunth (Lythraceae) Cultivated in Egypt. *J. Pharmacogn. Phytochem.* **2012**, *1*, 67−77.
(53) Guerrero, L.; Castillo, J.; Quiñones, M.; Garcia-Vallvé, S.; Arola, L.; Pujadas, G.; Muguerza, B. Inhibition of Angiotensin-Converting Enzyme Activity by Flavonoids: Structure-Activity Relationship Studies. *PLoS One* **2012**, *7*, No. e49493.
(54) Ahmad, I.; Mun'Im, A.; Luliana, S.; Elya, B.; Azminah, A.; Yanuar, A.; Artha, Y.; Negishi, O. Isolation, elucidation, and molecular docking studies of active compounds from Phyllanthus niruri with angiotensin-converting enzyme inhibition. *Pharmacogn. Mag.* **2018**, *14*, 604−610.
(55) Balasuriya, B. N.; Rupasinghe, H. V. Antihypertensive properties of flavonoid-rich apple peel extract. *Food Chem.* **2012**, *135*, 2320−2325.
(56) Lin, T.-c.; Hsu, F.-l.; Cheng, J.-T. Antihypertensive activity of corilagin and chebulinic acid, tannins from Lumnitzera, racemosa. *J. Nat. Prod.* **1993**, *56*, 629−632.
(57) Sieniawska, E. Activities of tannins−From *in vitro* studies to clinical trials. *Nat. Prod. Commun.* **2015**, No. 1934578X1501001118.

https://doi.org/10.1021/acsomega.2c05356
ACS Omega 2022, 7, 46524−46535